processes

Article

A Graphical User Interface for Calculating Exergy Destruction for Combustion Reactions

M. Özgün Korukçu

Department of Mechanical Engineering, University of Bursa Uludag, Gorukle, 16059 Bursa, Turkey;
ozkorukcu@uludag.edu.tr; Tel.: +90-2242941927

Abstract: The combustion of fuels has been studied by many researchers as it is used in a wide range of engineering applications. The chemical equilibrium approach served as the foundation for the investigation of combustion reactions. This article presents a software application designed to facilitate the calculation of combustion processes by calculating the combustion of 16 fuels among the common alkanes (C_nH_{2n+2}) and alcohols ($C_nH_{2n+1}OH$). The Ozan Combustion Calculator (OCC) offers a user-friendly and efficient graphical user interface (GUI) that allows users to easily input data and obtain results. The program was developed using MATLAB 2021a and LaTeX software, ensuring its reliability and accuracy. To perform these calculations, the program utilizes calculations of the thermophysical properties of fuels and water obtained from tables. The program consists of five modules, each serving a specific purpose. These modules calculate various parameters, such as the Adiabatic Flame Temperature, Exergy of Combustion with Dry Air, Exergy of Combustion with Moist Air, Energy of Combustion with Dry Air, and Energy of Combustion with Moist Air. Additionally, the program can be used to investigate the impact of relative humidity on the adiabatic flame temperature and exergy destruction. The results obtained from the calculations reveal that the adiabatic flame temperature exhibits a linear decrease as the relative humidity increases. On the other hand, exergy destruction demonstrates a quadratic increase with higher relative humidity values. The program derives mathematical relationships for the adiabatic flame temperature and exergy destruction with respect to relative humidity values, with a high regression coefficient ($r^2 = 0.999$). The versatility of OCC makes it suitable for various applications. It can be utilized in university settings for both undergraduate- and graduate-level courses, providing students with a practical tool for studying combustion processes. Additionally, it finds applications in industrial settings for the design and optimization of combustors, gas turbines, and burners. The user-friendly interface and accurate calculations make OCC a valuable resource in the field of combustion engineering.

Keywords: combustion; chemical equilibrium; fuel; adiabatic flame temperature; exergy

Citation: Korukçu, M.Ö. A Graphical User Interface for Calculating Exergy Destruction for Combustion Reactions. *Processes* **2024**, *12*, 294. https://doi.org/10.3390/pr12020294

Academic Editors: Dimitris Ipsakis and Andreas Yiotis

Received: 17 January 2024
Revised: 26 January 2024
Accepted: 27 January 2024
Published: 30 January 2024

1. Introduction

The utilization of energy heavily relies on the combustion of hydrocarbons, which can occur in liquid, solid, or gaseous states. This combustion process serves various purposes, including power generation, production within the process industry, heating systems for both residential and industrial use, implementation of safety measures, control of pollutant emissions, and active management of combustion processes [1]. In general, the primary parameter for premixed gases is the equivalence ratio (ϕ). When the equivalence ratio is greater than 1 ($\phi > 1$), it signifies rich combustion where the fuel is in excess. Conversely, a lean regime ($\phi < 1$) indicates that the oxidizer is in excess. Combustion in practical burners predominantly occurs at or below the stoichiometric mixture ratio ($\phi = 1$) [2]. In the field of combustion, the adiabatic flame temperature (AFT) holds great significance. It refers to the temperature at which the combustion process occurs adiabatically, without any heat transfer or alterations in kinetic or potential energy. In this context, the AFT represents the maximum temperature that the reactants can attain. However, it is important to emphasize that the highest AFT can only be achieved when the mixture is stoichiometric (ϕ = 1). To regulate the AFT, one can adjust the equivalence ratio (ϕ) to maintain the temperature values of the components within specific allowable limits [3]. AFT is directly influenced by pressure, the initial temperature, and the initial composition of the system [4].

In their study, Ufot et al. [5] investigated the AFT computations for gas turbine combustors employing conventional combustors. The analysis focused on a predetermined energy input and a stoichiometric ratio (ϕ) of 1.4. Glaude et al. [6] conducted a study to examine the utilization of biodiesels derived from rapeseed, soybean, and sunflower, as well as conventional fuels such as gas oil and natural gas. The focus of their investigation was to analyze the impact of these fuels on NOx emissions and the AFT. An analysis of the combustion products revealed that biodiesel products exhibit AFT and NOx indices that are comparable to those of gas oil but higher than those of natural gas. Kayadelen [7] conducted a study to examine the influence of natural gas components on the AFT, equilibrium products, and thermodynamics. The findings indicated that the AFT values were predominantly affected by CO_2, with isobutane (C_4H_{10}), propane (C_3H_8), and ethane (C_2H_6) also playing a role. Kayadelen [8] enhanced a comprehensive model to accurately predict the thermodynamic properties, AFT, and equilibrium products of various fuels, fuel blends, and additives. Law et al. [9] conducted a study to explore the potential enhancement of AFT values through off-stoichiometric combustion. The findings of their research indicated that a reduction in heat release, coupled with the occurrence of product dissociation peaks, leads to an increase in AFT values. In their study, Ozsari et al. [10] conducted a comparison of AFT, energy, and emission values for natural gas samples obtained from various countries, including Russia, the USA, Iran, and Australia. The researchers examined the performance of oxy-fuel combustion and conventional combustion with air for these natural gas samples. The findings of their investigation revealed that Russian natural gas exhibited the lowest emission values, while Australian natural gas demonstrated the lowest entropy production. The investigation conducted by Movileanu et al. [11] focused on analyzing the adiabatic flame temperature (AFT) of different fuel–air mixtures in combustion processes that were either isobaric or isochoric. The examination carried out by Sakhrieh [12] delved into the impact of the equivalence ratio, pressure, and initial temperature parameters on the AFT and laminar flame speed. The results of the study indicated that the optimal values for the AFT and laminar flame speed were attained when the equivalence ratio was maintained at ϕ = 1. In their study, Wu et al. [13] made significant advancements in a newly developed model aimed at determining the upper flammability limit of alkane combustion in the presence of air-CO_2 mixtures. To validate their model, the researchers conducted experiments utilizing mixtures of n-butane-CO_2 and n-isopentane-CO_2. An empirical model to calculate the heat of combustion of saturated carbons contained in power-generating fuels was conducted by Sagadeev and Sagadeev [14]. An additive scheme was used to compute the heat values of the fuels.

Numerous programs and methodologies are available for the determination of the AFT, energy, and chemical equilibrium in combustion processes. Reynolds made significant improvements to the STANJAN program by integrating the element potential method for the analysis of chemical equilibrium [15]. Furthermore, Gordon and McBride developed a computer program named CAE, which facilitates the calculation of complex chemical equilibrium compositions and their respective applications [16]. A computer program was introduced by Olikara [17] to facilitate the computation of the gas constant, enthalpy, and internal energy, as well as the partial derivatives of combustion products with temperature. On a different note, Eriksson developed a MATLAB graphical user interface (GUI) for a chemical equilibrium program. Program users can choose different fuels and products for combustion reactions. This program is designed to calculate the thermal properties of reactants and products involved in a combustion reaction [18]. By employing six major gas species and simplifying the governing equations into fourth-degree polynomials, Jarungthammachote successfully developed a quartic combustion model (QRC). This model allows for the determination of the AFT, molar fractions of combustion products, and properties [19]. GASEQ ver 0.79 is a software application that provides a solution for a range of calculations such as the AFT, compositions, adiabatic compression and expansions, equilibrium constants, and shock calculations [20]. The work of Frenklach et al. [21] highlights an optimized chemical reaction mechanism that pertains to the combustion of methane. By utilizing this model, one can effectively determine the ignition and flame properties associated with various methane combustion combinations. Cantera is a web-based application that computes the adiabatic flame temperature (AFT) based on the pressure, initial temperature, fuel type, and equivalence ratio [22]. EQLBRM, developed by Pratt [23], is a Fortran IV-based text-oriented program that draws inspiration from DOS/UNIX. Yazar and Demir [24] proposed a graphical user interface (GUI) for calculating the combustion, emission, and engine performance of internal combustion engines using the Java programming language. The effects of the in-cylinder pressure, temperature, mass ratios of gas components, and engine performance characteristics were obtained for different excess air ($\phi > 1$) ratios. Jakoubek et al. [25] developed online control algorithms to control flue gas emissions in power plants. The developed model is in communication with a real system to prevent unwanted emission values and to sustain energy production in power plants. Yildiz [26] used the chemical equilibrium-based combustion model and evaluated the effects of H_2 addition to biogases with different CO_2 contents. According to their study, the addition of H_2 increases the adiabatic flame temperature.

Efficiency evaluation of a thermal system heavily depends on the energy release derived from combustion. Although energy is predominantly employed in thermodynamic calculations and analyses, its quality cannot be adequately assessed solely based on these factors. The occurrence of irreversibilities during a process results in energy losses, consequently leading to the generation of entropy. Exergy, also known as available energy, holds significant importance in the design of thermal systems due to its association with exergy destruction or irreversibility [27]. The investigation carried out by Bouras and Khaldi focused on the exergy analysis of diverse fuel compositions. Their objective was to identify the ideal fuel composition that would result in both efficient combustion and economic benefits [28]. The exergy analysis performed by Koyun delved into the combustion of diverse octane and hydrogen blends within internal combustion engines. The study encompassed both complete and partial incomplete combustion scenarios, providing valuable insights into the energy efficiency of these processes [29]. Ozsari and Ust provided a detailed exergy analysis of the oxy-combustion process for diesel, gasoline, methane, and natural gas [30]. An exergy analysis of methane combustion was performed by Silva and Rouboa [31]. Som and Datta provided a comprehensive explanation regarding the occurrence of irreversibilities and exergy destruction during the combustion of gaseous, liquid, and solid fuels. Their study concluded that the primary cause of irreversibilities stemmed from the internal thermal exchange, which was directly associated with the presence of high-temperature gradients resulting from heat transfer in combustion reactions [32]. In their research, Taniguchi et al. [33] conducted a comprehensive investigation into the exergy and energy of combustion, power generation, and heat pump processes.

The present study aims to provide a comprehensive understanding of the combustion of alkanes and alcohols through the development of a graphical user interface (GUI) program. The developed program can calculate fuels of 12 alkanes (C_nH_{2n+2}) and 4 alcohols ($C_nH_{2n+1}OH$), which are not calculated in other programs. This program allows for the calculation of the AFT, energy, and exergy using both dry and moist air for a range of different fuels. Displaying the combustion equation on the screen, which was not available in previous studies, is an important feature.

Another aspect of this study involves investigating the correlation between the relative humidity and adiabatic flame temperature, as well as exergy destruction during combustion reactions. It is important to highlight that the impact of relative humidity on these parameters has not been thoroughly examined in previous research, as evidenced by the existing literature. Therefore, the present study aims to address this gap and contribute valuable insights to this research area.

2. Method

Within a combustion reaction, the fuel undergoes oxidation, resulting in the release of heat energy from the system. The primary oxidizer employed in this reaction is predominantly air. Air is modeled as a mixture of O_2 and 3.76 kmol of N_2. Combustion reactions of alkanes that are in the C_nH_{2n+2} form can be written for stoichiometric combustion ($\phi = 1$), rich combustion ($\phi > 1$), and excess air combustion ($\phi < 1$) as Equations (1)–(3).

$$C_nH_{2n+2} + \varnothing(O_2 + 3.76\ N_2)\ \rightarrow\ a\ CO_2 + b\ H_2O + c\ N_2\ \varnothing = 1 \tag{1}$$

$$C_nH_{2n+2} + \varnothing(O_2 + 3.76\ N_2)\ \rightarrow\ a\ CO_2 + b\ H_2O + c\ N_2 + d\ O_2\ \varnothing > 1 \tag{2}$$

$$C_nH_{2n+2} + \varnothing(O_2 + 3.76\ N_2)\ \rightarrow\ a\ CO_2 + b\ H_2O + c\ N_2 + d\ CO\ \varnothing < 1 \tag{3}$$

Combustion reactions of alcohols that are in the $C_nH_{2n+1}OH$ form are modeled in Equations (4) and (5).

$$C_nH_{2n+1}OH + \varnothing(O_2 + 3.76\ N_2)\ \rightarrow\ a\ CO_2 + b\ H_2O + c\ N_2\ \varnothing = 1 \tag{4}$$

$$C_nH_{2n+1}OH + \varnothing(O_2 + 3.76\ N_2)\ \rightarrow\ a\ CO_2 + b\ H_2O + c\ N_2 + d\ O_2\ \varnothing > 1 \tag{5}$$

The air–fuel ratio (AF) can be defined as the proportion of the mass of air (m_{air}) to the mass of fuel (m_{fuel}), as depicted in Equation (6).

$$AF = \frac{m_{air}}{m_{fuel}} \tag{6}$$

In cases where the air is not dry, the partial pressure of water vapor can be calculated by taking into account the relative humidity (φ_{air}) of the air and the saturation pressure at the given air temperature ($P_{sat@Tair}$).

$$P_{v,air} = \varphi_{air} P_{sat@Tair} \tag{7}$$

Under ideal gas assumptions, the mole number of moist air ($N_{v,air}$) can be found by using Equation (8).

$$N_{v,air} = \left(\frac{P_{v,air}}{P_{total}}\right) N_{total} \tag{8}$$

Combustion reactions of alkanes that are in the C_nH_{2n+2} form with moist air can be written for stoichiometric combustion ($\phi = 1$), rich combustion ($\phi > 1$), and excess air combustion ($\phi < 1$) as Equations (9)–(11).

$$C_nH_{2n+2} + \varnothing(O_2 + 3.76\ N_2) + N_{v,air}H_2O \rightarrow\ a\ CO_2 + b\ H_2O + c\ N_2\ \varnothing = 1 \tag{9}$$

$$C_nH_{2n+2} + \varnothing(O_2 + 3.76\ N_2) + N_{v,air}H_2O\ \rightarrow\ a\ CO_2 + b\ H_2O + c\ N_2 + d\ O_2\ \varnothing > 1 \tag{10}$$

$$C_nH_{2n+2} + \varnothing(O_2 + 3.76\ N_2) + N_{v,air}H_2O\ \rightarrow\ a\ CO_2 + b\ H_2O + c\ N_2 + d\ CO\ \varnothing < 1 \tag{11}$$

Combustion reactions of alcohols that are in the $C_nH_{2n+1}OH$ form with moist air are modeled in Equations (12) and (13).

$$C_nH_{2n+1}OH + \varnothing(O_2 + 3.76\ N_2) + N_{v,air}H_2O\ \rightarrow\ a\ CO_2 + b\ H_2O + c\ N_2\ \varnothing = 1 \tag{12}$$

$$C_nH_{2n+1}OH + \varnothing(O_2 + 3.76\ N_2) + N_{v,air}H_2O\ \rightarrow\ a\ CO_2 + b\ H_2O + c\ N_2 + d\ O_2\ \varnothing > 1 \tag{13}$$

According to the first law of thermodynamics, the steady-state energy balance can be written as Equation (14).

$$Q - W = \Delta H \tag{14}$$

The total enthalpy change between the reactants and products can be used to determine the energy released (Q_{out}) from the combustion system when there is no work present in the system. Equation (15) incorporates various factors such as the number of moles (N), the formation enthalpy ($\overline{h}^{\circ}_{for}$), the enthalpy of the component at a defined temperature ($\overline{h}_T$), and the reference enthalpy of the component at 1 atm and 25 °C ($\overline{h}^{\circ}_{ref}$).

$$Q_{out} = \underbrace{\sum N_R\left(\overline{h}^{\circ}_{for} + \overline{h}_T - \overline{h}^{\circ}_{ref}\right)_R}_{\substack{Energy\ in\ by\ mass \\ per\ mole\ of\ fuel}} - \underbrace{\sum N_P\left(\overline{h}^{\circ}_{for} + \overline{h}_T - \overline{h}^{\circ}_{ref}\right)_P}_{\substack{Energy\ out\ by\ mass \\ per\ mole\ of\ fuel}} \tag{15}$$

$$Q = W = 0 \tag{16}$$

In an adiabatic combustion process, the enthalpies of reactants (H_R) and products (H_P) will be equal, as expressed in Equations (17) and (18).

$$H_R = H_P \tag{17}$$

Equation (18) shows the energy balance between reactants and products. By using Equation (18), the enthalpy of the products ($\overline{h}_{T,P}$) and the adiabatic flame temperature (T_{af}) can be found. Since there is only one equation and multiple unknowns, T_{af} can be solved by trial and error or numerically.

$$\sum N_R\left(\overline{h}^{\circ}_{for} + \overline{h}_T - \overline{h}^{\circ}_{ref}\right)_R = \sum N_P\left(\overline{h}^{\circ}_{for} + \overline{h}_T - \overline{h}^{\circ}_{ref}\right)_P \tag{18}$$

The net change in the entropy of a system can be calculated with Equation (19).

$$\underbrace{S_{in} - S_{out}}_{\substack{Net\ entropy \\ transfer\ by \\ heat\ and\ mass}} + \underbrace{S_{gen}}_{\substack{Entropy \\ generation}} = \underbrace{\Delta S_{system}}_{\substack{Change\ in \\ entropy}} \tag{19}$$

The entropy generation for closed or steady-flow systems can be found in Equation (20).

$$S_{gen} = S_P - S_R + \sum \frac{Q_{out}}{T_{ambient}} \tag{20}$$

If the process is adiabatic ($Q_{out} = 0$), Equation (21) can be used.

$$S_{gen,\ adiabatic} = S_P - S_R \geq 0 \tag{21}$$

In the context of the combustion reaction, both the reactants and products are considered to be ideal gas mixtures. The entropy per mole ($\overline{s}_n$) for any component within the mixture can be determined using Equation (22). This equation takes into account various factors, including the absolute entropy ($\overline{s}^{\circ}_n$); the universal gas constant (R_u), which is typically valued at 8.3144 7 kJ/kmol K; the mole fraction of the component (y_n); the total pressure of the mixture (P_m); and the pressure of the ambient environment ($P_{ambient}$).

$$\overline{s}_n(T, P_n) = \overline{s}^{\circ}_n(T, P_0) - R_u ln \frac{y_n P_m}{P_{ambient}} \tag{22}$$

The entropy of a component can be found in Equation (23). Here, N_n is the mole number of the component.

$$S_n = N_n \overline{s}_n(T, P_n) = N_n\left[\overline{s}^{\circ}_n(T, P_0) - R_u ln \frac{y_n P_m}{P_{ambient}}\right] \tag{23}$$

Using Equations (21)–(23), entropy generation is obtained as in Equation (24).

$$S_{gen} = \sum N_P \bar{s}_P - \sum N_R \bar{s}_R + \sum \frac{Q_{out}}{T_{ambient}} \tag{24}$$

The exergy destruction in the combustion system can be found in Equation (25).

$$X_{destroyed} = T_{ambient}\, S_{gen} \tag{25}$$

Equations (1)–(25) were taken from Cengel and Boles [27].

The following assumptions were made in the calculations in this study:

- The air and products involved in the combustion process are considered to be ideal gases.
- The pressure during combustion and the pressure of the surrounding environment remain constant.

Figure 1 illustrates the flow diagram of the AFT calculation. Once the fuel type and equivalence ratio are selected, the program proceeds to calculate the combustion equilibrium constants and calculate enthalpy values [27,34]. Subsequently, the initial guess for the AFT is obtained, followed by another enthalpy calculation retrieval and the actual AFT calculation. If the calculated error falls below the tolerance limit ($\Delta\varepsilon = 1 \times 10^{-15}$), the program terminates the loop and displays the results on the screen.

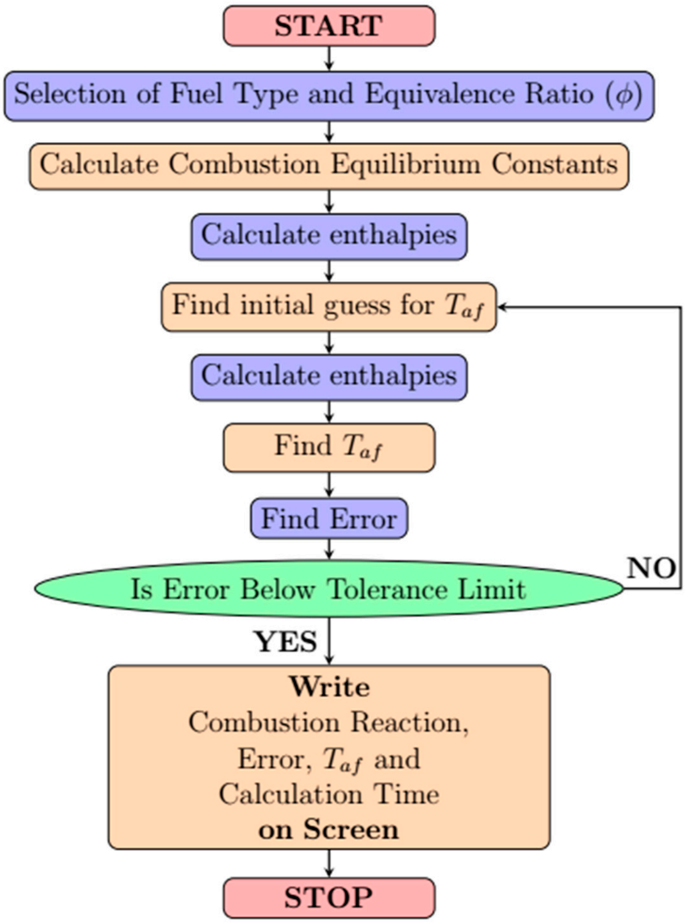

Figure 1. Flow diagram of adiabatic flame temperature (AFT) calculation.

The flow diagram depicted in Figure 2 provides a visual representation of the steps involved in calculating the AFT and conducting exergy analysis for dry and moist air. The AFT calculation procedure remains unchanged from the first flow diagram. However, when dealing with moist air, the temperature of the air (T_{air}) and the relative humidity ratio of the air (φ_{air}) are selected as initial parameters. Tables are then consulted to determine the moles of water vapor. Following the AFT calculation, the program proceeds to compute the entropy generation and exergy destruction and ultimately displays the results on the screen.

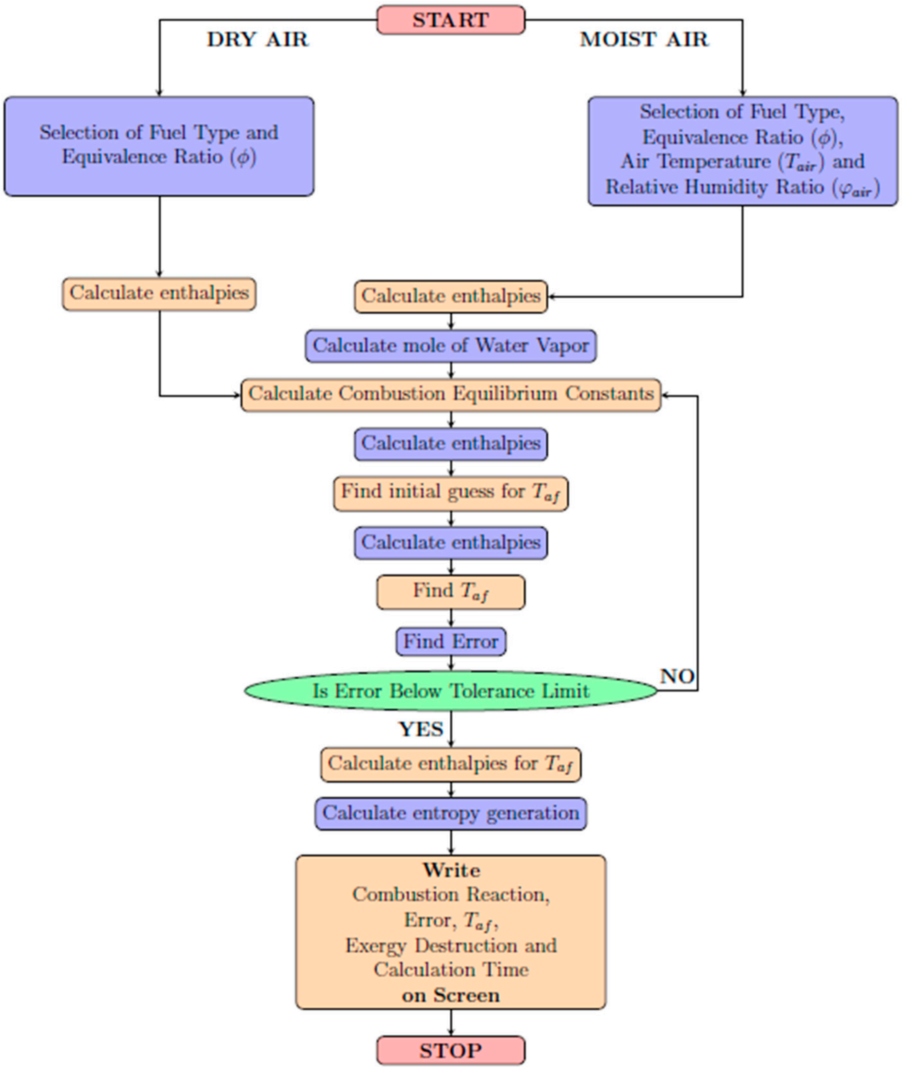

Figure 2. Flow diagram of adiabatic flame temperature (AFT) calculation and exergy analysis for dry and moist air.

Figure 3 depicts a flow diagram illustrating the process of conducting energy and exergy analyses for both dry and moist air. The user is required to make several selections and input various parameters. These include choosing the fuel type, specifying the equivalence ratio (ϕ), providing the air temperature (T_{air}), indicating the relative humidity ratio of the air (φ_{air}), and, if moist air is being used, entering the mass flow rate of fuel and the combustion temperature. In the case of moist air, additional steps are taken. Tables are consulted to determine the mole number of water vapor, which is then calculated. Subsequently, the combustion equilibrium constants are computed, followed by the determination of the energy, exergy destruction, air–fuel ratio, and mass flow rate of air. Finally, the obtained results are displayed on the screen.

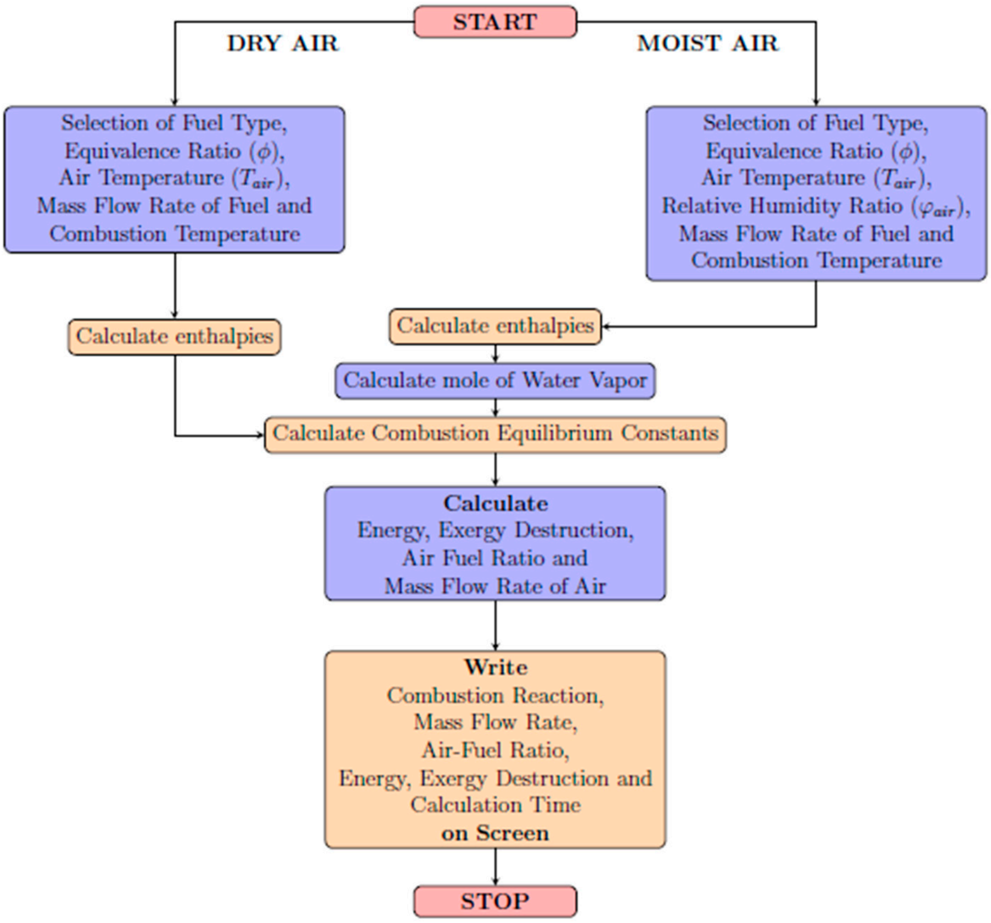

Figure 3. Flow diagram of energy and exergy analyses for dry and moist air.

3. Verification of the Calculations

The software was validated by calculating the adiabatic flame temperature of liquid octane ($C_8H_{18\ (liquid)}$) combustion for stoichiometric combustion ($\phi = 1$), rich combustion ($\phi > 1$), and excess air combustion ($\phi < 1$). The stoichiometric combustion ($\phi = 1$) of liquid ethanol ($C_2H_5OH_{\ (liquid)}$) was compared with experimental data [35]. The validation results are presented in Table 1.

Table 1. Comparison of adiabatic flame temperature values with Refs. [3,35]
.

Fuel	Equivalence Ratio	Ref. [3]	Ref. [27]	Ref. [35]	Present Study	Error (%)
$C_8H_{18\ (liquid)}$	$\phi = 0.9$	-	2395 K	-	2394.5 K	0.02
$C_8H_{18\ (liquid)}$	$\phi = 1$	-	2286 K	-	2285.9 K	0.004
$C_8H_{18\ (liquid)}$	$\phi = 4$	961.8 K	962 K	-	962.03 K	0.003
$C_2H_5OH_{\ (liquid)}$	$\phi = 1$	-	-	2242 K	2292 K	2.2

The adiabatic flame temperature and exergy destruction for the combustion of methane (CH_4) at 25 °C and 1 atm with an equivalence ratio of $\phi = 1.5$ were compared with those given by the developed software, and the results are presented in Table 2.

Table 2. Comparison of adiabatic flame temperature and exergy destruction values with Ref. [3].

Fuel	Equivalence Ratio	Ref. [3]	Present Study	Error (%)
		Adiabatic Flame Temperature		
CH_4	ϕ = 1.5	1789 K	1789.04 K	0.002
		Exergy Destruction		
CH_4	ϕ = 1.5	288,000 kJ/kmol	288,247 kJ/kmol	0.08

The heat transfer rate and exergy destruction for the combustion of liquid propane ($C_3H_{8(liquid)}$) at 25 °C and 0.4 kg/min mass flow rate with air at 12 °C and an equivalence ratio of ϕ = 2.5 were compared with those given by the developed software, and the results are presented in Table 3.

Table 3. Comparison of heat transfer rate and exergy destruction values with Ref. [3].

Fuel	Equivalence Ratio	Ref. [3]	Present Study	Error (%)
		Heat Transfer Rate		
$C_3H_{8(liquid)}$	ϕ = 2.5	28.853 kJ/s	28.858 kJ/s	0.017
		Exergy Destruction		
$C_3H_{8(liquid)}$	ϕ = 2.5	1,120,510 kJ/kmol	1,118,672 kJ/kmol	0.16

As can be seen from Tables 1–3, the results from the Ozan Combustion Calculator (OCC) are in good agreement with the results obtained from references. In light of these results, it can be concluded that the developed graphical user interface (GUI) exhibits a high level of accuracy and reliability.

4. Implementation

The primary interface of the OCC program empowers users to select one of five problems through its main screen. Figure 4 visually presents this main screen, where users can conveniently choose their desired problem to calculate. The selection of fuels is made by using the predefined list of fuels. In addition to fuel selection, users are prompted to input various parameters, including the equivalence ratio (ϕ), air temperature (T_{air}), relative humidity ratio of the air (φ_{air}), mass flow rate of fuel, and combustion temperature. Figure 5 showcases the comprehensive list of fuels available in the AFT calculation program.

Figure 6 shows the results from the AFT calculation of liquid octane ($C_8H_{18\ (liquid)}$) combustion with an equivalence ratio of ϕ = 1.5 (Adiabatic Flame Temperature Calculation Module).

Figure 7 shows the AFT result and exergy analysis of benzene (C_6H_6) combustion with an equivalence ratio of ϕ = 1 (Adiabatic Flame Temperature and Exergy Calculation Module).

The AFT result and exergy analysis of butane (C_4H_{10}) combustion with an equivalence ratio of ϕ = 0.8 at 300 K and $\varphi_{air} = 0.9$ is presented in Figure 8 (Adiabatic Flame Temperature of Combustion With Moist Air and Exergy Calculation Module).

In Figure 9, energy and exergy analyses of methyl alcohol (CH_3OH) combustion with an equivalence ratio of ϕ = 1.2 at 288 K, fuel mass flow rate of 12 kg/s, and combustion temperature of 1250 K are presented (Energy and Exergy Module).

Figure 10 shows the results of energy and exergy analyses of ethyl alcohol (C_2H_5OH) combustion with an equivalence ratio of ϕ = 1.2 at 300 K and $\varphi_{air} = 0.95$, fuel mass flow rate of 5 kg/s, and combustion temperature of 1250 K (Fuel Combustion With Moist Air Energy and Exergy Calculation Module).

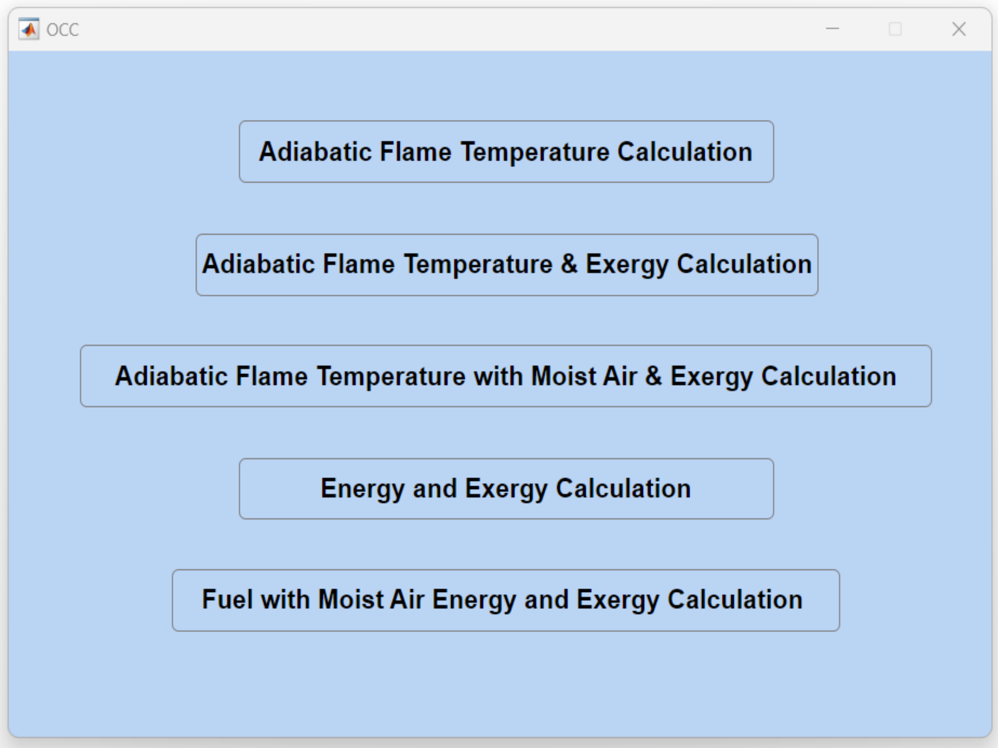

Figure 4. The main screen of the OCC.

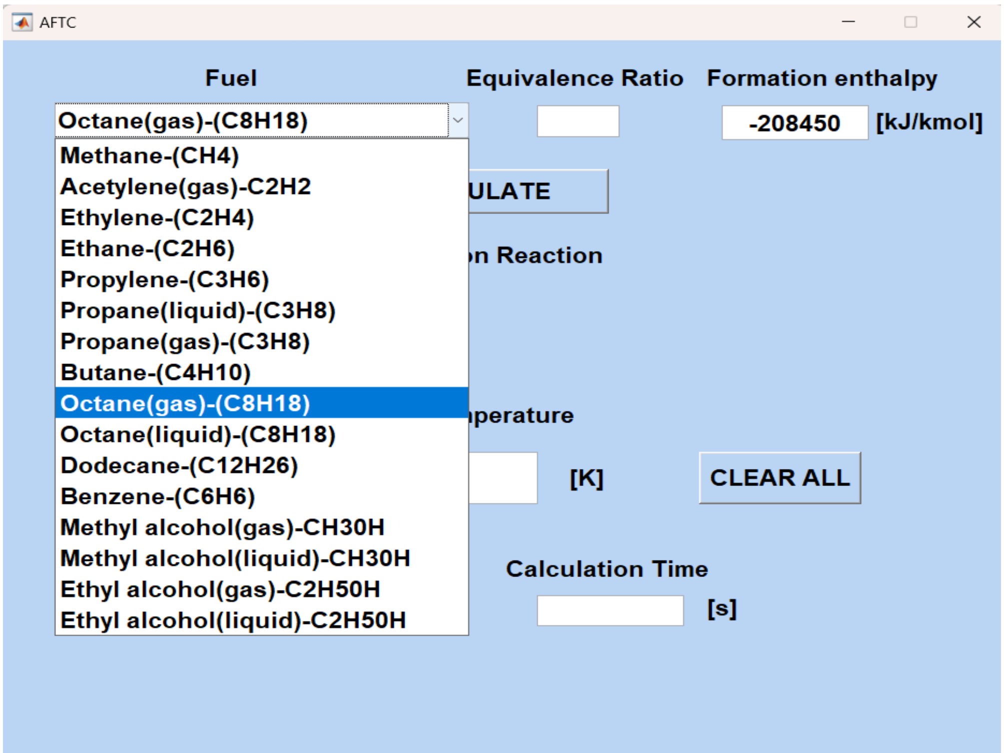
Fuel: Octane(gas)-(C8H18)

Formation enthalpy: -208450 [kJ/kmol]

Figure 5. Selection of fuels from the AFT calculation program.

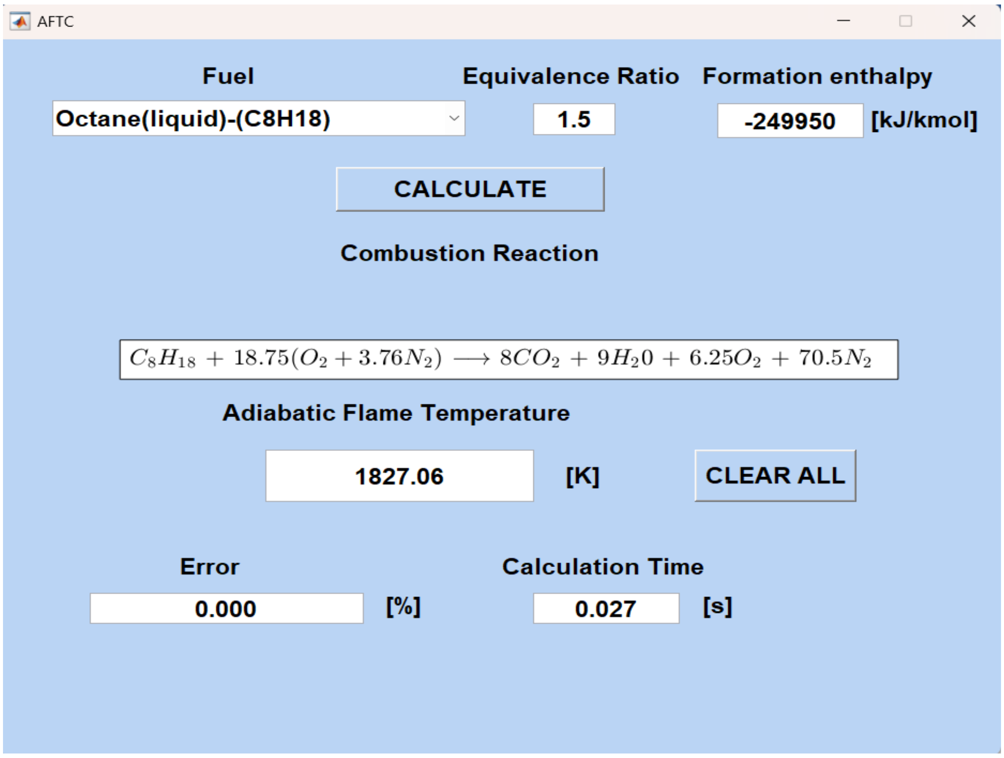

Fuel: Octane(liquid)-(C8H18)

Equivalence Ratio: 1.5

Formation enthalpy: -249950 [kJ/kmol]

Combustion Reaction

$$C_8H_{18} + 18.75(O_2 + 3.76N_2) \longrightarrow 8CO_2 + 9H_20 + 6.25O_2 + 70.5N_2$$

Adiabatic Flame Temperature: 1827.06 [K]

Error: 0.000 [%]

Calculation Time: 0.027 [s]

Figure 6. AFT calculation of liquid octane ($C_8H_{18\ (liquid)}$) combustion with an equivalence ratio of $\phi = 1.5$.

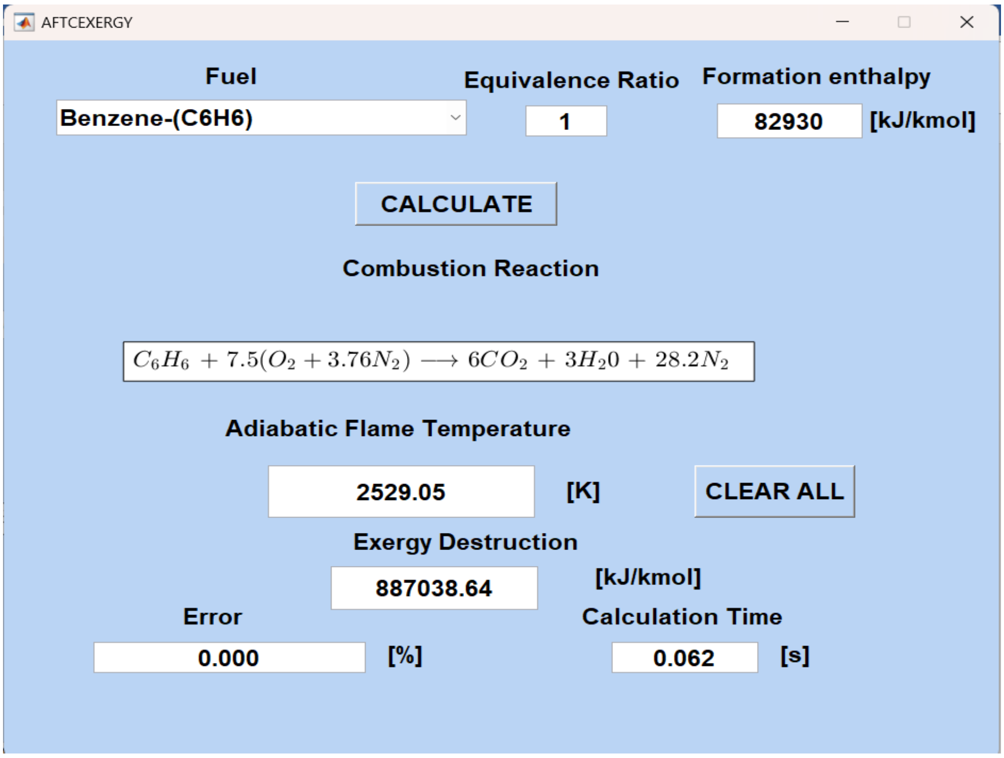

Fuel: Benzene-(C6H6)

Equivalence Ratio: 1

Formation enthalpy: 82930 [kJ/kmol]

Combustion Reaction

$$C_6H_6 + 7.5(O_2 + 3.76N_2) \longrightarrow 6CO_2 + 3H_20 + 28.2N_2$$

Adiabatic Flame Temperature: 2529.05 [K]

Exergy Destruction: 887038.64 [kJ/kmol]

Error: 0.000 [%]

Calculation Time: 0.062 [s]

Figure 7. AFT and exergy analysis of benzene (C_6H_6) combustion with an equivalence ratio of $\phi = 1$.

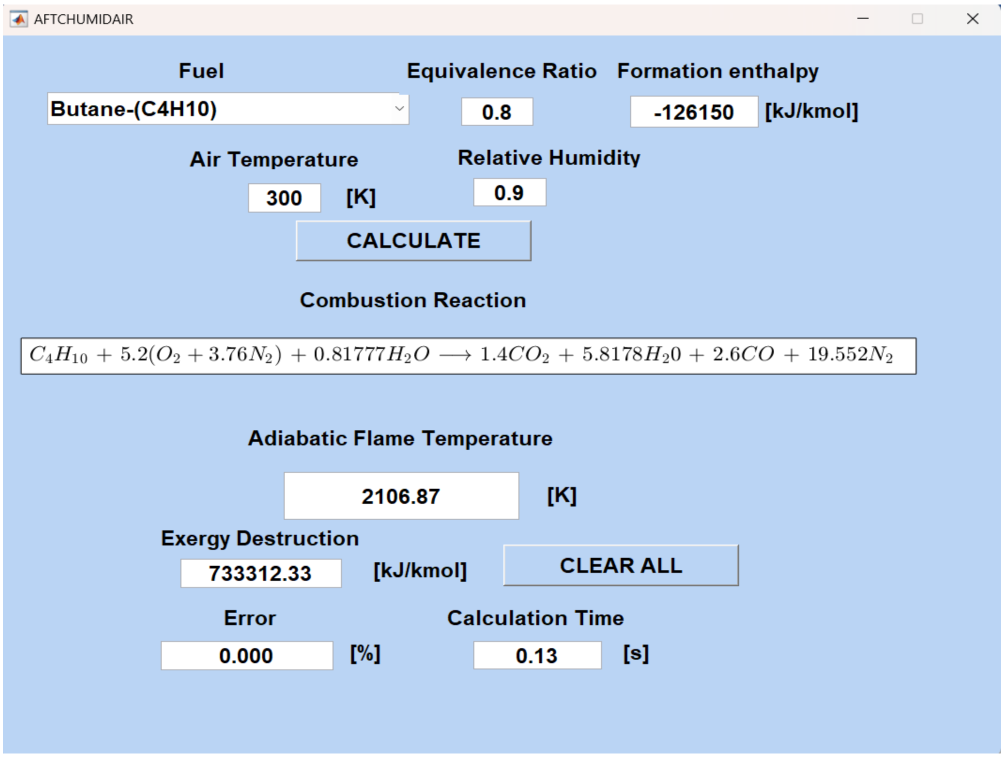

Fuel: Butane-(C4H10)
Equivalence Ratio: 0.8
Formation enthalpy: -126150 [kJ/kmol]
Air Temperature: 300 [K]
Relative Humidity: 0.9

Combustion Reaction

$$C_4H_{10} + 5.2(O_2 + 3.76N_2) + 0.81777H_2O \longrightarrow 1.4CO_2 + 5.8178H_20 + 2.6CO + 19.552N_2$$

Adiabatic Flame Temperature: 2106.87 [K]
Exergy Destruction: 733312.33 [kJ/kmol]
Error: 0.000 [%]
Calculation Time: 0.13 [s]

Figure 8. AFT and exergy analysis of butane (C_4H_{10}) combustion with an equivalence ratio of ϕ = 0.8 at 300 K and $\varphi_{air} = 0.9$.

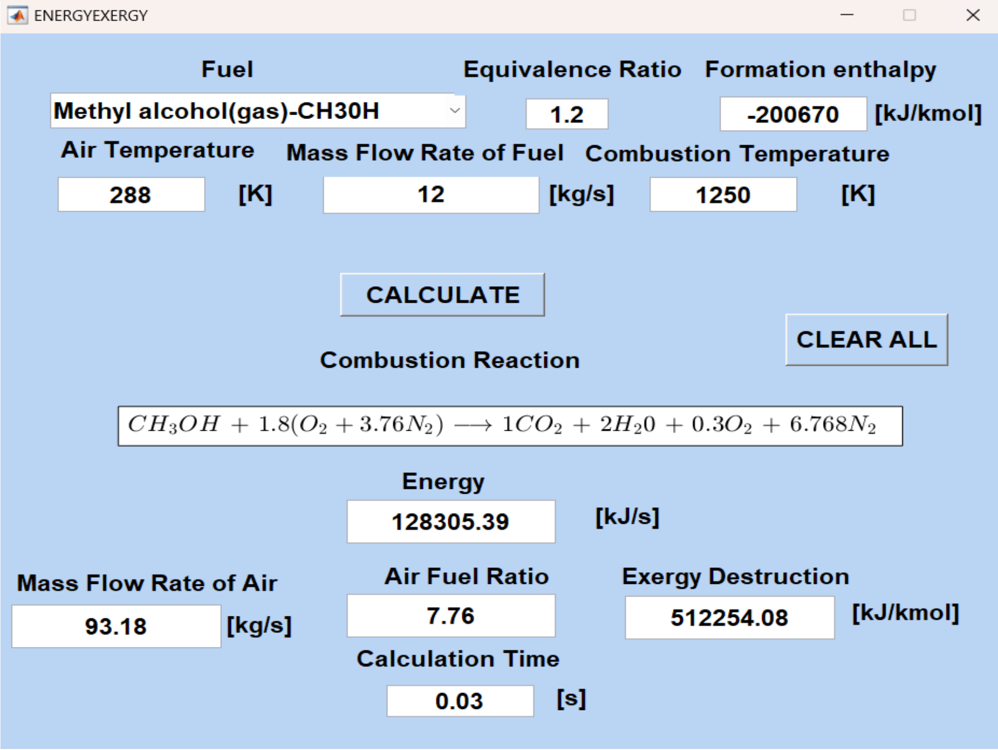

Fuel: Methyl alcohol(gas)-CH30H
Equivalence Ratio: 1.2
Formation enthalpy: -200670 [kJ/kmol]
Air Temperature: 288 [K]
Mass Flow Rate of Fuel: 12 [kg/s]
Combustion Temperature: 1250 [K]

Combustion Reaction

$$CH_3OH + 1.8(O_2 + 3.76N_2) \longrightarrow 1CO_2 + 2H_20 + 0.3O_2 + 6.768N_2$$

Energy: 128305.39 [kJ/s]
Mass Flow Rate of Air: 93.18 [kg/s]
Air Fuel Ratio: 7.76
Exergy Destruction: 512254.08 [kJ/kmol]
Calculation Time: 0.03 [s]

Figure 9. Energy and exergy analyses of methyl alcohol (CH_3OH) combustion with an equivalence ratio of ϕ = 1.2 at 288 K and a fuel mass flow rate of 12 kg/s.

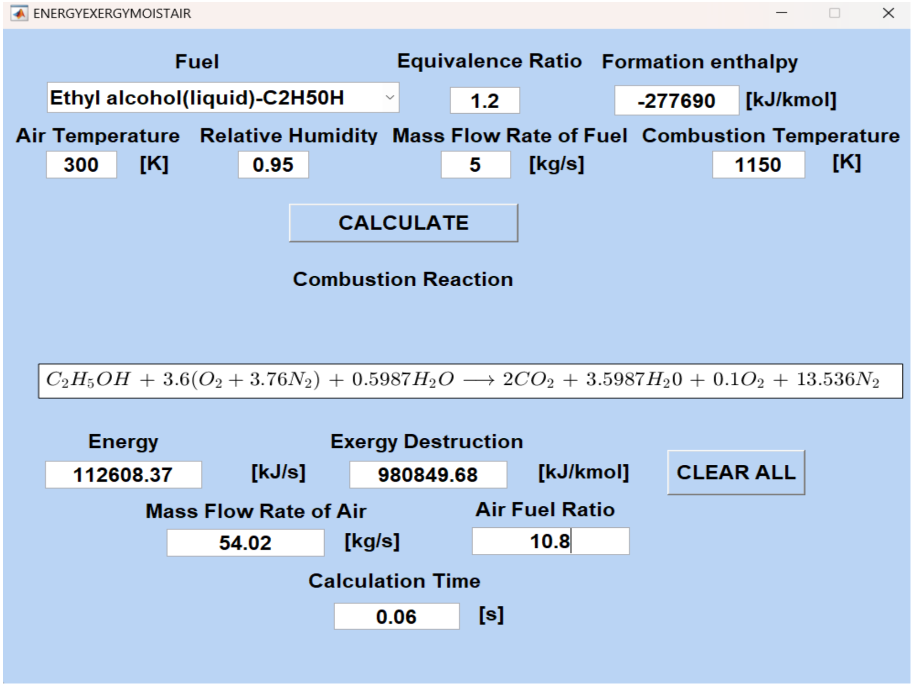

Fuel: Ethyl alcohol(liquid)-C2H50H

Equivalence Ratio: 1.2

Formation enthalpy: -277690 [kJ/kmol]

Air Temperature: 300 [K]

Relative Humidity: 0.95

Mass Flow Rate of Fuel: 5 [kg/s]

Combustion Temperature: 1150 [K]

Combustion Reaction

$$C_2H_5OH + 3.6(O_2 + 3.76N_2) + 0.5987H_2O \longrightarrow 2CO_2 + 3.5987H_20 + 0.1O_2 + 13.536N_2$$

Energy: 112608.37 [kJ/s]

Exergy Destruction: 980849.68 [kJ/kmol]

Mass Flow Rate of Air: 54.02 [kg/s]

Air Fuel Ratio: 10.8

Calculation Time: 0.06 [s]

Figure 10. Energy and exergy analyses of ethyl alcohol (C_2H_5OH) combustion with an equivalence ratio of ϕ = 1.2 at 300 K and $\varphi_{air} = 0.95$, with a fuel mass flow rate of 5 kg/s.

5. Effect of Relative Humidity on Adiabatic Flame Temperature and Exergy Destruction

This study aimed to examine the impact of relative humidity on the adiabatic flame temperature and exergy destruction in combustion systems. The calculations were conducted while keeping the equivalence ratio at 1 and the air temperature at 300 K. Figure 11 provides a graphical representation of the variations in adiabatic flame temperature with the relative humidity for all the fuels analyzed in this research.

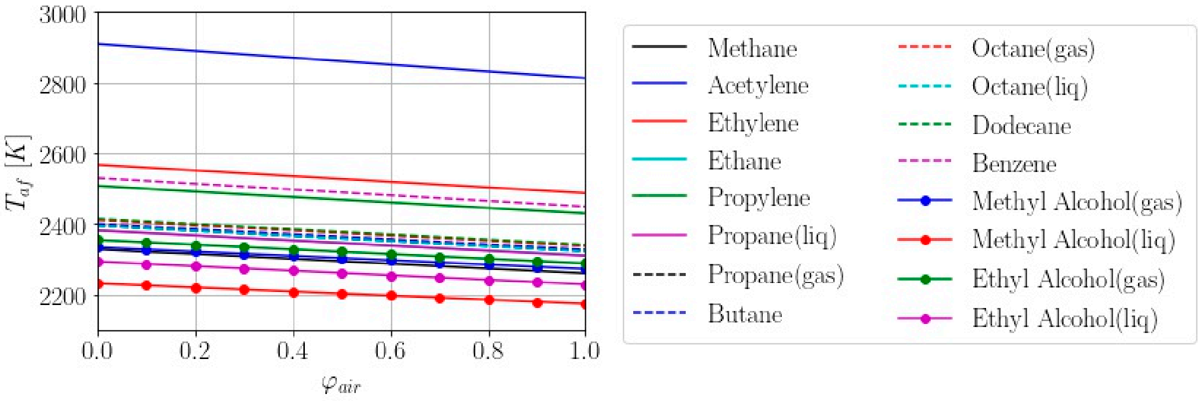

Figure 11. Variation in the adiabatic flame temperature (AFT) with relative humidity (φ_{air}).

The derivation of an equation to express the change in adiabatic flame temperature (AFT) with relative humidity (φ_{air}) was accomplished through the application of linear regression analysis. The findings from both Figure 11 and Equation (21) demonstrate a clear negative linear relationship between the adiabatic flame temperature (AFT) and relative humidity (φ_{air}). The coefficients of Equation (26), which are specific to the fuels examined in this study, are provided in Table 4.

$$T_{af} = a\varphi_{air} + b \tag{26}$$

Table 4. Coefficients for Equation (26).

Fuel	*a*	*b*	r^2
Methane (CH_4)	−68.284	2328.5	0.999
Acetylene (C_2H_2)	−96.605	2909.7	0.999
Ethylene (C_2H_4)	−80.18	2567.7	0.999
Ethane (C_2H_6)	−71.182	2382	0.999
Propylene (C_3H_6)	−77.774	2507.7	0.999
Propane (Liquid) (C_3H_8)	−72.011	2381.7	0.999
Propane (Gas) (C_3H_8)	−72.534	2395.6	0.999
Butane (C_4H_{10})	−72.946	2400.5	0.999
Octane (Gas) (C_8H_{18})	−73.701	2411.1	0.999
Octane (Liquid) (C_8H_{18})	−73.123	2395.6	0.999
Dodecane ($C_{12}H_{26}$)	−73.967	2414.8	0.999
Benzene (C_6H_6)	−80.915	2530.2	0.999
Methyl Alcohol (Gas) (CH_3OH)	−61.366	2334.1	0.999
Methyl Alcohol (Liquid) (CH_3OH)	−57.982	2231.9	0.999
Ethyl Alcohol (Gas) (C_2H_5OH)	−66.645	2354.8	0.999
Ethyl Alcohol (Liquid) (C_2H_5OH)	−64.404	2293.5	0.999

Another expression for exergy destruction ($X_{destroyed}$) variation during the combustion of the studied fuels with relative humidity (φ_{air}) is given in Equation (27). According to Equation (27), there is a quadratic positive correlation between exergy destruction ($X_{destroyed}$) and relative humidity (φ_{air}). The coefficients of Equation (27) are represented in Table 5.

$$X_{destroyed} = c\varphi_{air}{}^2 + d\varphi_{air} + e \tag{27}$$

Table 5. Coefficients for Equation (27).

Fuel	*c*	*d*	*e*	r^2
Methane (CH_4)	1187.1	2067.5	235,602	0.999
Acetylene (C_2H_2)	1442.5	4584.1	284,419	0.999
Ethylene (C_2H_4)	1780.5	4137.2	354,237	0.999
Ethane (C_2H_6)	2075.4	3967	428,564	0.999
Propylene (C_3H_6)	2683.4	5959.5	543,265	0.999
Propane (Liquid) (C_3H_8)	2958.2	5794.6	639,774	0.999
Propane (Gas) (C_3H_8)	2972.4	5831.9	621,081	0.999
Butane (C_4H_{10})	3881.4	7678.6	813,235	0.999
Octane (Gas) (C_8H_{18})	7431	15220	2,000,000	0.999
Octane (Liquid) (C_8H_{18})	7392.8	15087	2,000,000	0.999
Dodecane ($C_{12}H_{26}$)	10964	22786	2,000,000	0.999
Benzene (C_6H_6)	4271.5	11620	887,039	0.999
Methyl Alcohol (Gas) (CH_3OH)	896.75	1439.9	214,778	0.999
Methyl Alcohol (Liquid) (CH_3OH)	887.72	1318.1	243,462	0.999
Ethyl Alcohol (Gas) (C_2H_5OH)	1826.9	3163.6	404,904	0.999
Ethyl Alcohol (Liquid) (C_2H_5OH)	1793.9	3044.4	435,784	0.999

6. Conclusions

A novel software application, utilizing a graphical user interface (GUI), was developed to facilitate the analysis of combustion processes based on chemical equilibrium. This software offers users the ability to compute the adiabatic flame temperature and determine the equilibrium products resulting from the combustion of commonly used alkanes and alcohols. Notably, this software surpasses its predecessors by providing a visual representation of the combustion equation directly on the screen, a feature that was previously unavailable in combustion calculation software. Furthermore, the software's functionality extends to calculating the energy released to the ambient surroundings and evaluating the exergy destruction associated with the combustion reaction.

This study also delved into the influence of relative humidity on the adiabatic flame temperature and exergy destruction. The results indicate a negative linear correlation between relative humidity and the adiabatic flame temperature. Furthermore, a positive quadratic relationship was identified between exergy destruction and relative humidity. The expressions describing the adiabatic flame temperature and exergy destruction with respect to relative humidity demonstrate a strong correlation coefficient value (r^2 = 0.999).

The easy-to-use graphical interface allows the user to control the input parameters to see the combustion equation and the analysis results. It is also helpful for lecturers when teaching the subject of combustion, giving homework, and preparing or correcting for exams.

This software application is suitable for implementation in both undergraduate- and graduate-level courses that encompass combustion reactions. The utilization of this program effectively reduces the occurrence of calculation errors. Furthermore, the fuel library within the program can be expanded to include additional fuel blends and incorporate other functionalities, thereby paving the way for potential commercialization in the future. Moreover, this program finds applications in various industrial sectors, such as the design of combustion chambers, internal combustion engines, gas turbines, and burners.

Funding: This research received no external funding.

Data Availability Statement: Data are contained within the article.

Conflicts of Interest: The author declares no conflict of interest.

Nomenclature

AF	Air–fuel ratio
$\bar{h}^{\circ}_{for}$	Formation enthalpy (kJ/kmol)
$\bar{h}^{\circ}_{ref}$	Reference enthalpy (kJ/kmol)
$\bar{h}_T$	Enthalpy at given temperature (kJ/kmol)
$\boldsymbol{H}$	Enthalpy (kJ)
$\boldsymbol{m_{air}}$	Mass of air (kg)
$\boldsymbol{m_{fuel}}$	Mass of fuel (kg)
N	Mole number of component
$\boldsymbol{N_{total}}$	Total mole number
$\boldsymbol{N_{v,air}}$	Mole number of moist air
$\boldsymbol{P_{total}}$	Total pressure (kPa)
$\boldsymbol{P_{v,air}}$	Partial pressure of water vapor (kPa)
$\boldsymbol{Q}$	Heat energy (kJ)
$\boldsymbol{R_u}$	Universal gas constant (kJ/kmol K)
$\bar{s}^{\circ}_n$	Absolute entropy (kJ/kmol K)
$\boldsymbol{S}$	Entropy (kJ/K)
T	Temperature (K)
$\boldsymbol{W}$	Mechanical energy (kJ)
$\boldsymbol{y_n}$	Mole fraction of component
X	Exergy destruction (kJ/kmol)
Greek Letters	
$\boldsymbol{\varphi}$	Relative humidity
ϕ	Equivalence ratio
Subscripts	
gen	Generated
n	Component
R	Reactants
P	Products

References

1. Kuo, K.K. *Principles of Combustion*; John Wiley&Sons, Inc.: Hoboken, NJ, USA, 2005.
2. Poinsot, T.; Veynante, D. *Theoretical and Numerical Combustion*, 2nd ed.; RT Edwards, Inc.: Morningside, Australia, 2005; Volume 53.
3. Van Wylen, G.J.; Borgnakke, C.; Sonntag, R.E. *Fundamentals of Thermodynamics*; Wiley, John Wiley&Sons, Inc.: Hoboken, NJ, USA, 2009.
4. Williams, F.A. *Combustion Theory*; CRC Press: Boca Raton, FL, USA, 1985.
5. Ufot, E.; Lebele-Alawa, B.T.; Douglas, I.E. On the adiabatic flame temperature in gas-turbine combustors. *Eur. J. Sci. Res.* **2011**, *64*, 387–393.
6. Glaude, P.A.; Fournet, R.; Bounaceur, R.; Molière, M. Adiabatic flame temperature from biofuels and fossil fuels and derived effect on NOx emissions. *Fuel Process. Technol.* **2010**, *91*, 229–235. [CrossRef]
7. Kayadelen, H.K. Effect of natural gas components on its flame temperature, equilibrium combustion products and thermodynamic properties. *J. Nat. Gas Sci. Eng.* **2017**, *45*, 456–473. [CrossRef]
8. Kayadelen, H.K. A multi-featured model for estimation of thermodynamic properties, adiabatic flame temperature and equilibrium combustion products of fuels, fuel blends, surrogates and fuel additives. *Energy* **2018**, *143*, 241–256. [CrossRef]
9. Law, C.K.; Makino, A.; Lu, T.F. On the off-stoichiometric peaking of adiabatic flame temperature. *Combust. Flame* **2006**, *145*, 808–819. [CrossRef]
10. Ozsari, I.; Ust, Y.; Kayadelen, H.K. Comparative Energy and Emission Analysis of Oxy-Combustion and Conventional Air Combustion. *Arab. J. Sci. Eng.* **2021**, *46*, 2477–2492. [CrossRef]
11. Movileanu, C.; Mitu, M.; Brinzea, V.; Musuc, A.; Mocanu, M.; Razus, D.; Oancea, D. Adiabatic flame temperature of fuel-air mixtures in isobaric and isochoric combustion processes. *Rev. Chim.* **2011**, *62*, 376–379.
12. Sakhrieh, A. The adiabatic flame temperature and laminar flame speed of methane premixed flames at varying pressures. *Acta Period. Technol.* **2019**, *50*, 220–227. [CrossRef]
13. Wu, M.; Shu, G.; Chen, R.; Tian, H.; Wang, X.; Wang, Y. A new model based on adiabatic flame temperature for evaluation of the upper flammable limit of alkane-air-CO_2 mixtures. *J. Hazard. Mater.* **2018**, *344*, 450–457. [CrossRef]
14. Sagadeev, E.V.; Sagadeev, V.V. Calculation of the heats of combustion of aromatic hydrocarbons contained in power-generating fuel. *High Temp.* **2006**, *44*, 530–534. [CrossRef]
15. Reynolds, W.C. *The Element Potential Method for Chemical Equilibrium Analysis: Implementation in the Interactive Program STANJAN*; Stanford University: Stanford, CA, USA, 1986.
16. Gordon, S.; McBride, B.J. *Computer Program for Calculation of Complex Chemical Equilibrium Compositions and Applications I. Analysis*; NASA RP-1311; NASA: Washington, DC, USA, 1994; p. 58.
17. Olikara, C.; Borman, G.L. A computer program for calculating properties of equilibrium combustion products with some applications to I.C. engines. *SAE Tech. Pap.* **1975**, 7191. [CrossRef]
18. Eriksson, L. CHEPP—A chemical equilibrium program package for Matlab. *SAE Tech. Pap.* **2004**, *113*, 730–741. [CrossRef]
19. Jarungthammachote, S. Simplified model for estimations of combustion products, adiabatic flame temperature and properties of burned gas. *Therm. Sci. Eng. Prog.* **2020**, *17*, 100393. [CrossRef]
20. Morley, C. Gaseq Chemical Equilibrium Program. Available online: http://www.gaseq.co.uk/ (accessed on 15 December 2023).
21. Frenklach, M.; Wang, H.; Goldenberg, M.; Smith, G.P.; Golden, D.M.; Bowman, C.T.; Hanson, R.K.; Gardiner, W.C.; Lissianski, V. *GRI-Mech—An Optimized Detailed Chemical Reaction Mechanism for Methane Combustion*; SRI International: Menlo Park, CA, USA, 1995.
22. Cantera. Available online: http://elearning.cerfacs.fr/combustion/tools/adiabaticflametemperature/index.php (accessed on 15 December 2023).
23. Pratt, D.T. Available online: https://aste-classes.usc.edu/utility/flame_temperature.php (accessed on 15 December 2023).
24. Yazar, O.; Demir, B. Development of the Software Program That Can Account the Combustion, Emission and Engine Performance Values of Internal Combustion Engines. *Eur. J. Technol.* **2022**, *12*, 129–138. [CrossRef]
25. Jakoubek, P.; Hanzal, L. Matlab As a Tool for Fossil Fuel Power Plant Combustion Control. Available online: https://dsp.vscht.cz/konference_matlab/MATLAB10/full_text/044_Jakoubek.pdf (accessed on 15 December 2023).
26. Yıldız, M. Chemical equilibrium based combustion model to evaluate the effects of H_2 addition to biogases with different CO_2 contents. *Int. J. Hydrogen Energy* **2023**, *52*, 1334–1344. [CrossRef]
27. Cengel, Y.; Boles, M.A. *Thermodynamics an Engineering Approach*, 5th ed.; McGraw-Hill: New York, NY, USA, 2011.
28. Bouras, F.; Khaldi, F. Optimization of Combustion Efficiency Using a Fuel Composition Based on CH_4 and/or H_2. *Russ. J. Appl. Chem.* **2020**, *93*, 1954–1959. [CrossRef]
29. Koyun, T. Exergy Analysis of Different Blends of Hydrogen and Octane for Combustion Conditions of Internal Combustion Engine. *J. Nanoelectron. Optoelectron.* **2018**, *13*, 1656–1668. [CrossRef]
30. Ozsari, I.; Ust, Y. Effect of varying fuel types on oxy-combustion performance. *Int. J. Energy Res.* **2019**, *43*, 8684–8696. [CrossRef]
31. Silva, V.; Rouboa, A. Methane combustion: An exergy analysis. *AIP Conf. Proc.* **2011**, *1389*, 179–182. [CrossRef]
32. Som, S.K.; Datta, A. Thermodynamic irreversibilities and exergy balance in combustion processes. *Prog. Energy Combust. Sci.* **2008**, *34*, 351–376. [CrossRef]
33. Taniguchi, H.; Mouri, K.; Nakahara, T.; Arai, N. Exergy analysis on combustion and energy conversion processes. *Energy* **2005**, *30*, 111–117. [CrossRef]

34. Stull, D.R.; Prophet, H. *JANAF Thermochemical Tables*, 2nd ed.; National Institute of Standards and Technology: Gaithersburg, MD, USA, 1971.
35. Zhou, J.; Lu, C.; Xu, C.; Yu, Z. Experimental and Numerical Study on the Effect of Hydrogen Addition on Laminar Burning Velocity of Ethanol–Air Mixtures. *Energies* **2022**, *15*, 3114. [CrossRef]